

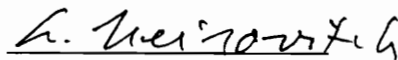
INFLUENCE OF BASE ISOLATION ON THE RESPONSE OF STRUCTURES TO EARTHQUAKES

by
César Augusto Morales Velasco

Thesis submitted to Faculty of the
Virginia Polytechnic Institute and State University
in partial fulfillment of the requirements for the degree of

Master of Science
in
Engineering Mechanics

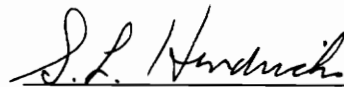
Approved:



L. Meirovitch, Chairman



R. Heller



S. Hendricks

July 1995
Blacksburg, Virginia

C.2

LD
5055
V855
1995
M669
C.2

INFLUENCE OF BASE ISOLATION ON THE RESPONSE OF STRUCTURES TO EARTHQUAKES

by

César Augusto Morales Velasco

Dr. Leonard Meirovitch, Chairman
Engineering Mechanics

ABSTRACT

In this thesis, the seismic analysis of base isolated structures is carried out using a base coordinate relative to the inertial space that renders absolute dynamic response, which is fundamental in assessing base isolation. Moreover, the structure is modeled as an Euler-Bernoulli beam cantilevered on a massive basement. The isolation system is modeled as linear. The stochastic analysis is carried out in the frequency domain using a stationary Clough-Penzien spectral representation for the ground excitation. Standard deviations of the structure's generalized coordinates and their second derivatives are obtained, which characterize the response, including stresses, of the structure. The effectiveness of base isolation can be evaluated by comparing the response of the isolated structure with the nonisolated counterpart. The results show that base isolation is highly effective in reducing the overall response of the structure. Additionally, it is found that the Clough-Penzien representation does not model adequately in the high frequency range. A modification of this model is proposed.

ACKNOWLEDGMENTS

I would like to express immense gratitude to my advisor, Dr. Leonard Meirovitch, for his academic guidance and support. I express also eternal gratitude to Universidad Simón Bolívar, Fundación Sivensa and Fundación Gran Mariscal de Ayacucho, all in Venezuela, for the support that made possible my graduate studies.

Thanks are also due to the Engineering Science and Mechanics Department, for an outstanding education; specially, Dr. Robert Heller and Dr. Scott Hendricks, excellent educators, for their support as members of the graduate committee

I would like to thank my parents, Agustín Morales and Virginia Velasco for their support and encouragement throughout my academic career.

TABLE OF CONTENTS

ABSTRACT	
ACKNOWLEDGMENTS	iii
LIST OF FIGURES	v
LIST OF TABLES	vi
NOMENCLATURE	vii
1. INTRODUCTION	1
2. EQUATIONS OF MOTION	2
2.1 Mathematical Model	2
2.2 Equations of motion	2
3. RESPONSE TO HARMONIC EXCITATION	8
3.1 Analysis	8
3.2 Comparative Analysis of Isolated and Unisolated Structure Response	10
4. RESPONSE TO RANDOM EXCITATION	15
4.1 Analysis	15
4.2 Comparative Analysis of Isolated and Unisolated Structure Response	19
5. SUMMARY AND SUGGESTIONS FOR FURTHER WORK	31
5.1 Summary	31
5.2 Suggestions for Further Work	32
REFERENCES	33
VITA	34

LIST OF FIGURES

2.1	Physical model for the base isolated building	3
2.2	Mechanical Model	4
3.1	Amplitude parameter R as a function of base mass	13
4.1	Ground acceleration power spectral density function	20
4.2	Force power spectral density function	21
4.3	Squared magnitude of H_{11}	22
4.4	Squared magnitude of H_{12}	22
4.5	Integrand for the base displacement standard deviation	23
4.6	Integrand for the first modal amplitude standard deviation	23
4.7	Integrand for the second modal amplitude standard deviation	24
4.8	Integrand for the third modal amplitude standard deviation	24
4.9	Integrand for the fourth modal amplitude standard deviation	25
4.10	Integrand for the base acceleration standard deviation	25
4.11	Integrand for the standard deviation of \ddot{q}_2	26
4.12	Integrand for the first modal amplitude standard deviation (unisolated)	26
4.13	Integrand for the second modal amplitude standard deviation (unisolated)	27
4.14	Integrand for the third modal amplitude standard deviation (unisolated)	27
4.15	Integrand for the fourth modal amplitude standard deviation (unisolated)	28
4.16	Integrand for the standard deviation of \ddot{s}_1 (unisolated)	28
4.17	Integrand for the standard deviation of \ddot{s}_2 (unisolated)	29

LIST OF TABLES

3.1 Parameters of the mechanical model of the building	11
3.2 Modal parameters of the building	12
3.3 Results of the amplitude parameters Ra_i and Rb_j	13
4.1 Standard deviation of the generalized displacements	29
4.2 Standard deviation of the generalized accelerations	29
4.3 Standard deviation of the generalized displacements (double ζ)	30
4.2 Standard deviation of the generalized accelerations (double ζ)	30

NOMENCLATURE

k	Rubber bearing stiffness constant
c	Hydraulic damper viscous damping coefficient
M	Base mass
m	Linear density of the building
E	Young's modulus of the building
I	Cross-section area moment of inertia
L	Building's height
X	Axis fixed to the inertial space
x	Axis fixed to the base
$y(x,t)$	Base-relative displacement of the building
$u(t)$	Horizontal displacement of the ground
$r(t)$	Horizontal displacement of the base
t	Time
T	Kinetic energy
V	Potential energy
W_{nc}	Nonconservative work
t_1, t_2	Arbitrary instants of time
$s(t)$	Modal amplitude vector
$Y_j(x)$	Cantilever beam eigenfunctions
n	Number of considered beam modes
C_j	Eigenfunction amplitude coefficients
A_j, B_j	Eigenfunction constants
β_j	Eigenfunction differential equation coefficients
ω_j	Cantilever beam natural frequencies
δ_{jk}	Kronecker delta
$\mathbf{q}(t)$	Generalized coordinate vector
M	Mass matrix
C	Damping matrix
K	Stiffness matrix

$\mathbf{f}(t)$	Force vector
$M_o(x,t)$	Flexural moment
U	Ground harmonic amplitude
ω	Harmonic excitation frequency (Chapter 3) and frequency (Chapter 4)
\mathbf{F}	Harmonic force amplitude vector
\mathbf{Q}	Generalized coordinate amplitude vector (harmonic)
D	Impedance matrix
m_{ij}	Matrix D minor determinants
R	Dimensionless harmonic amplitude parameter
ϕ	Phase angle
\mathbf{v}	Vector independent of M, c, k
Rb_j	Harmonic amplitude parameter (unisolated)
a, b	Coefficients independent of M, c, k
Ra_i	Harmonic amplitude parameter
$\mathbf{x}(t)$	State space vector
A	State space matrix
B	State space matrix
I	Identity matrix
O	Zero matrix
\mathbf{m}_x	State space vector mean
$\Phi(t)$	Transition matrix
\mathbf{m}_f	Force vector mean
$\mathbf{m}_{\ddot{q}}$	Acceleration vector mean
$S_{xx}(\omega)$	State space vector power spectral density matrix
$H(\omega)$	Frequency response matrix
$S_{ff}(\omega)$	Force power spectral density matrix
$R_{ff}(\tau)$	Force correlation matrix
$S_{f_1 f_1}(\omega)$	Force power spectral density function
$R_{f_1 f_1}(\tau)$	Force autocorrelation function
$R_{\dot{u}\dot{u}}(\tau)$	Ground velocity autocorrelation function
$R_{uu}(\tau)$	Ground displacement autocorrelation function
$R_{\dot{u}u}(\tau)$	Ground velocity-displacement cross correlation function
$S_{\dot{u}\dot{u}}(\omega)$	Ground velocity power spectral density function
$S_{uu}(\omega)$	Ground displacement power spectral density function

$S_{\ddot{u}u}(\omega)$	Ground velocity-displacement cross power spectral density function
$S_{\ddot{u}\ddot{u}}(\omega)$	Ground acceleration power spectral density function
ζ_g	Ground filter damping factor
ω_g	Ground filter natural frequency
ζ_c	Second filter parameter
ω_c	Second filter parameter
S_0	White noise signal intensity
σ_i	Generalized coordinate standard deviation
σ_{a_i}	Generalized acceleration standard deviation
$\mathbf{x}_j(t)$	State space vector (unisolated)
A_j	State space matrix (unisolated)
B_j	State space matrix (unisolated)
$\mathbf{f}_j(t)$	Generalized force (unisolated)
$\mathbf{m}_{\mathbf{x}_j}$	State space vector mean (unisolated)
$\Phi_j(t)$	Transition matrix (unisolated)
$\mathbf{m}_{\mathbf{f}_j}$	Force mean value (unisolated)
$\mathbf{m}_{\ddot{\mathbf{s}}}$	Acceleration vector mean (unisolated)
$S_{\mathbf{x}_j\mathbf{x}_j}(\omega)$	State space vector power spectral density matrix (unisolated)
$H_j(\omega)$	Frequency response matrix (unisolated)
$S_{\mathbf{f}_j\mathbf{f}_j}(\omega)$	Force power spectral density function (unisolated)
$R_{\mathbf{f}_j\mathbf{f}_j}(\tau)$	Force autocorrelation function (unisolated)
$R_{\ddot{u}\ddot{u}}(\tau)$	Ground acceleration autocorrelation function
σ_u	Ground displacement standard deviation
$\sigma_{\ddot{u}}$	Ground acceleration standard deviation

1.- INTRODUCTION

Current earthquake engineering practice is to build very strong, well supported structures capable of resisting moderate earthquakes through plastic deformations. Failure of some structural members is sometimes tolerated. However, such designs tend to be expensive and disastrous in major earthquakes. Therefore, new approaches are imperative.

Base isolation is a novel engineering technique for improving the overall performance of structures during earthquakes. The simple idea behind this technology is to isolate the structure from the moving ground through flexible mountings so as to reduce the dynamic response and internal forces in structures.

Base isolation was developed mainly empirically. Pioneers in the field used mainly one degree of freedom models, with the displacement measured with respect to a reference frame attached to the moving ground. The mechanical models have been improved, but the ground-based reference frame is still used. With the early models, the shifting of the “structure’s natural frequency” away from the excitation spectral band, due to the added flexibility, was the reason for the reduced (relative) response. Lately, the focus is on reducing the response by increasing the dissipative characteristics of the isolation system.

In this work, we analyze and compare the response of isolated and unisolated structures subjected to earthquakes. Because the objectives of earthquake engineering are 1) to prevent injury to the occupants and damage to the contents and 2) to protect the integrity of the structure, while keeping the amplitudes of motion at reasonable levels, comparison criteria are based on absolute displacement and acceleration amplitudes and stress levels in the structure.

Because the idea is to stabilize the base relative to the inertial space, an inertial-based reference frame is used. The analysis is performed modeling the structure as a continuous flexural beam. The beam is cantilevered from a large lumped mass acting as the base.

The equations of motion of the structure are derived in Chapter 2. In Chapter 3, we first obtain the response to harmonic excitation. Then, in Chapter 4, which represents the core of this work, we address the actual stochastic problem.

2. EQUATIONS OF MOTION

2.1 Mathematical Model

Civil structures tend to be very complex, not easy to model. Mathematical models must consider the essential dynamic characteristics. Clearly, what is essential and what can be ignored often depends on the effects to be studied.

Most research on the response of structures to earthquakes has been carried out using lumped-parameter models, with the mass concentrated in the floors and the stiffness in the walls. More sophisticated models include the continuous shear beam. In this study, we model the structure as an Euler-Bernoulli uniform beam. This model is superior, as it regards the mass and stiffness properties as distributed. The effect of the floors can be added later as lumped masses in a more refined continuous model. One of the advantages of this model is that not only the internal shear but also the flexural moment can be calculated; it is well known that the moment is more critical than the shearing force in beams. The internal damping, inherently nonviscous, tends to be low, so that it is ignored.

Several devices for base isolation have been proposed and a complete review has been done by Kelly (Ref. 1). We perform the analysis for the rubber bearing type which are the most used in base isolated buildings. As we show later, damping is important in reducing the response. Because damping provided by the rubber pads is very low, it is necessary to add other damping mechanisms. We carry out the analysis with hydraulic dampers. A complete description of these devices can be found in Ref. 2. The physical model for the base isolated building is drawn in Fig. 2.1 which includes a massive base whose influence is studied.

We idealize the isolation system as a spring with elastic constant k and a dashpot with viscous coefficient c which act horizontally. Thus, the mechanical model is depicted in Fig. 2.2 in which M is the mass of the base while m , E , I and L represent the linear density, Young's modulus, section moment of inertia and height of the uniform beam, respectively.

2.2 Equations of Motion

The equations of motion are obtained by means of the extended Hamilton's

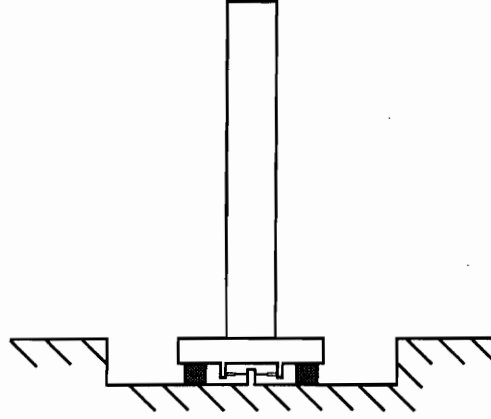


Figure 2.1 Physical model for the base isolated building

principle (Ref. 3). To this end, we refer to Fig. 2.2 where X is an axis fixed to the inertial space and x is an axis fixed to the base. We denote by $u(t)$ the absolute ground displacement, by $r(t)$ the absolute displacement of the base from its original position and by $y(x,t)$ the elastic deformation of the beam relative to x . This definition of base coordinate is not the one commonly used in the analysis of base isolated structures; most of the work in this field is done using the relative displacement of the base, which leads to the paradox that the structure is stabilized relative to the moving ground, instead to the inertial space.

The kinetic energy of the system is

$$T = \frac{1}{2} M \dot{r}^2 + \frac{1}{2} m \int_0^L \left(\dot{r} + \frac{\partial y}{\partial t} \right)^2 dx \quad (2.1)$$

and the potential energy is

$$V = \frac{1}{2} k (r - u)^2 + \frac{1}{2} EI \int_0^L \left(\frac{\partial^2 y}{\partial x^2} \right)^2 dx \quad (2.2)$$

The variation in the kinetic energy has the form

$$\begin{aligned} \delta T &= M r \delta \dot{r} + m \int_0^L \left(\dot{r} + \frac{\partial y}{\partial t} \right) \left(\delta \dot{r} + \delta \frac{\partial y}{\partial t} \right) dx \\ &= M r \delta \dot{r} + m \int_0^L \left[\dot{r} \delta \dot{r} + \frac{\partial y}{\partial t} \delta \dot{r} + \left(\dot{r} + \frac{\partial y}{\partial t} \right) \delta \frac{\partial y}{\partial t} \right] dx \end{aligned} \quad (2.3)$$

and the variation in the potential energy is simply

$$\delta V = k (r - u) \delta r + EI \int_0^L \frac{\partial^2 y}{\partial x^2} \delta \frac{\partial^2 y}{\partial x^2} dx \quad (2.4)$$

Moreover, the nonconservative virtual work of the system is

$$\delta W_{nc} = -c (\dot{r} - \dot{u}) \delta r \quad (2.5)$$

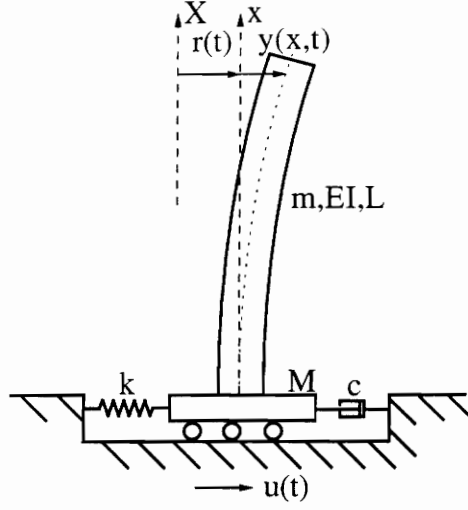


Figure 2.2 Mechanical model

The extended Hamilton's principle can be written as

$$\int_{t_1}^{t_2} (\delta T - \delta V + \delta W_{nc}) dt = 0 \quad , \delta r = \delta y = 0 \text{ at } t = t_1, t_2 \quad (2.6)$$

where t_1 and t_2 are arbitrary times. Introduction of Eqs. (2.3), (2.4) and (2.5) into Eq. (2.6) leads to

$$\int_{t_1}^{t_2} \left[(M + mL) \dot{r} \delta \dot{r} + m \int_0^L \frac{\partial y}{\partial t} \delta \dot{r} dx + m \int_0^L \left(\dot{r} + \frac{\partial y}{\partial t} \right) \delta \frac{\partial y}{\partial t} dx + k(u - r) \delta r - EI \int_0^L \frac{\partial^2 y}{\partial x^2} \delta \frac{\partial^2 y}{\partial x^2} dx + c(\dot{u} - \dot{r}) \delta r \right] dt = 0 \quad (2.7)$$

The variation and differentiation processes are interchangeable, so that we can write

$$\begin{aligned} \int_{t_1}^{t_2} (M + mL) \dot{r} \frac{d\delta r}{dt} dt &= (M + mL) (\dot{r} \delta r) \Big|_{t_1}^{t_2} - \int_{t_1}^{t_2} \ddot{r} \delta r dt \\ \int_{t_1}^{t_2} \frac{\partial y}{\partial t} \frac{d\delta r}{dt} dt &= \frac{\partial y}{\partial t} \delta r \Big|_{t_1}^{t_2} - \int_{t_1}^{t_2} \frac{\partial^2 y}{\partial t^2} \delta r dt \\ \int_{t_1}^{t_2} \left(\dot{r} + \frac{\partial y}{\partial t} \right) \frac{\partial \delta y}{\partial t} dt &= \left(\dot{r} + \frac{\partial y}{\partial t} \right) \delta y \Big|_{t_1}^{t_2} - \int_{t_1}^{t_2} \left(\ddot{r} + \frac{\partial^2 y}{\partial t^2} \right) \delta y dt \\ \int_0^L \frac{\partial^2 y}{\partial x^2} \frac{\partial^2 \delta y}{\partial x^2} dx &= \frac{\partial^2 y}{\partial x^2} \delta \frac{\partial y}{\partial x} \Big|_0^L - \int_0^L \frac{\partial^3 y}{\partial x^3} \frac{\partial \delta y}{\partial x} dx = \frac{\partial^2 y}{\partial x^2} \delta \frac{\partial y}{\partial x} \Big|_0^L - \frac{\partial^3 y}{\partial x^3} \delta y \Big|_0^L + \int_0^L \frac{\partial^4 y}{\partial x^4} \delta y dx \end{aligned} \quad (2.8)$$

Introducing Eqs. (2.8) into Eq. (2.7), we obtain

$$\int_{t_1}^{t_2} \left[-(M + mL)\ddot{r} + c(\dot{u} - \dot{r}) + k(u - r) - m \int_0^L \frac{\partial^2 y}{\partial t^2} dx \right] \delta r + \int_0^L \left\{ -m(\ddot{r} + \frac{\partial^2 y}{\partial t^2}) - EI \frac{\partial^4 y}{\partial x^4} \right\} \delta y \, dx - EI \frac{\partial^2 y}{\partial x^2} \delta \frac{\partial y}{\partial x} \Big|_0^L + EI \frac{\partial^3 y}{\partial x^3} \delta y \Big|_0^L \, dt = 0 \quad (2.9)$$

The virtual displacements δr , δy and $\delta \frac{\partial y}{\partial x}$ are arbitrary and independent, so that, using the standard arguments of the calculus of variations, we obtain the differential equations

$$-(M + mL)\ddot{r} - m \int_0^L \frac{\partial^2 y}{\partial t^2} dx + c(\dot{u} - \dot{r}) + k(u - r) = 0 \quad (2.10)$$

$$m(\ddot{r} + \frac{\partial^2 y}{\partial t^2}) + EI \frac{\partial^4 y}{\partial x^4} = 0 \quad (2.11)$$

and the boundary conditions

$$\frac{\partial^2 y}{\partial x^2} \delta \frac{\partial y}{\partial x} \Big|_0^L = 0 \quad , \quad \frac{\partial^3 y}{\partial x^3} \delta y \Big|_0^L = 0 \quad (2.12 \text{ a,b})$$

Considering the system geometry, Eqs. (2.12) lead to the boundary conditions

$$y = 0 \quad , \quad \frac{\partial y}{\partial x} = 0 \quad \text{at} \quad x = 0 \quad (2.13 \text{ a,b})$$

$$\frac{\partial^2 y}{\partial x^2} = 0 \quad , \quad \frac{\partial^3 y}{\partial x^3} = 0 \quad \text{at} \quad x = L \quad (2.13 \text{ c,d})$$

Because boundary conditions (2.13) are those of a cantilever beam, we express the elastic deformation in the form (Ref. 3)

$$y(x, t) = \sum_{j=1}^n s_j(t) Y_j(x) \quad (2.14)$$

where s_j are modal amplitudes and Y_j are the cantilever beam eigenfunctions (Ref. 4)

$$Y_j(x) = \frac{C_j}{A_j} [A_j(\sin \beta_j x - \sinh \beta_j x) + B_j(\cos \beta_j x - \cosh \beta_j x)] \quad (2.15)$$

where

$$A_j = \sin \beta_j L - \sinh \beta_j L \quad , \quad B_j = \cos \beta_j L + \cosh \beta_j L \quad (2.16)$$

in which $\beta_j L$ are roots of the characteristic equation

$$\cos \beta_j L \cosh \beta_j L = -1 \quad (2.17)$$

We determine C_j such that the functions are not only orthogonal but also orthonormal, or (Ref. 4)

$$\int_0^L m Y_j(x) Y_k(x) dx = \delta_{jk} \quad (2.18)$$

in which case we also have that

$$\int_0^L EI Y_j(x) \frac{d^4 Y_k(x)}{dx^4} dx = \omega_j^2 \delta_{jk} \quad (2.19)$$

where

$$\omega_j = \beta_j^2 \sqrt{\frac{EI}{m}} \quad (2.20)$$

are the cantilever beam natural frequencies.

Next, we insert Eq (2.14) into Eqs. (2.10) and (2.11), multiply the second by Y_k and integrate over x and obtain the discretized equations of motion

$$m \sum_{j=1}^n \ddot{s}_j(t) \int_0^L Y_j(x) dx + (M + mL)\ddot{r} + c\dot{r} + kr = c\dot{u} + ku \quad (2.21)$$

$$\ddot{s}_j(t) + \omega_j^2 s_j(t) = -m\ddot{r} \int_0^L Y_j(x) dx \quad (2.22)$$

It is not difficult to show that

$$\int_0^L Y_j(x) dx = \frac{2C_j}{\beta_j} \quad (2.23)$$

So that the equations of motion, Eqs. (2.21) and (2.22) can be expressed in the matrix form

$$M\ddot{\mathbf{q}} + C\dot{\mathbf{q}} + K\mathbf{q} = \mathbf{f} \quad (2.24)$$

where

$$\mathbf{q} = \begin{pmatrix} r \\ s_1 \\ \vdots \\ s_{n-1} \\ s_n \end{pmatrix}, \quad \mathbf{f} = \begin{pmatrix} c\dot{u} + ku \\ 0 \\ \vdots \\ 0 \\ 0 \end{pmatrix} \quad (2.25 \text{ a,b})$$

are the configuration vector and force vector, and

$$M = \begin{pmatrix} M + mL & 2mC_1/\beta_1 & \cdots & 2mC_{n-1}/\beta_{n-1} & 2mC_n/\beta_n \\ 2mC_1/\beta_1 & 1 & \cdots & 0 & 0 \\ \vdots & \vdots & \ddots & \vdots & \vdots \\ 2mC_{n-1}/\beta_{n-1} & 0 & \cdots & 1 & 0 \\ 2mC_n/\beta_n & 0 & \cdots & 0 & 1 \end{pmatrix}$$

$$C = \begin{pmatrix} c & 0 & \cdots & 0 & 0 \\ 0 & 0 & \cdots & 0 & 0 \\ \vdots & \vdots & \ddots & \vdots & \vdots \\ 0 & 0 & \cdots & 0 & 0 \\ 0 & 0 & \cdots & 0 & 0 \end{pmatrix} \quad K = \begin{pmatrix} k & 0 & \cdots & 0 & 0 \\ 0 & \omega_1^2 & \cdots & 0 & 0 \\ \vdots & \vdots & \ddots & \vdots & \vdots \\ 0 & 0 & \cdots & \omega_{n-1}^2 & 0 \\ 0 & 0 & \cdots & 0 & \omega_n^2 \end{pmatrix} \quad (2.26 \text{ a,b,c})$$

are the mass, damping and stiffness matrices.

In the case of an unisolated cantilevered structure, $r=u$ and the equation of motion for the beam can be obtained from Eq. (2.11) in the form

$$m \frac{\partial^2 y}{\partial t^2} + EI \frac{\partial^4 y}{\partial x^4} = -m\ddot{u} \quad (2.27)$$

Using Eq. (2.14), Eq (2.27) becomes

$$m \sum_{j=1}^n Y_j(x) \ddot{s}_j(t) + EI \sum_{j=1}^n s_j(t) \frac{d^4 Y_j(x)}{dx^4} = -m\ddot{u} \quad (2.28)$$

Multiplying by Y_k , integrating over x and using Eq.(2.23), the discretized equations of motion can be written as

$$\ddot{s}_j + \omega_j^2 s_j = -\frac{2mC_j}{\beta_j} \ddot{u} \quad , \quad j=1,2,\dots,n \quad (2.29)$$

We notice that they are uncoupled.

The stresses in the structure are related to the bending moment which is given by

$$M_o(x,t) = EI \frac{\partial^2 y(x,t)}{\partial x^2} \quad (2.30)$$

which, upon substitution of Eq. (2.14), becomes

$$M_o(x,t) = EI \sum_{j=1}^n s_j(t) \frac{d^2 Y_j(x)}{dx^2} \quad (2.31)$$

3. RESPONSE TO HARMONIC EXCITATION

3.1 Analysis

Before we study the response to actual earthquake excitation, we propose to study the effect of the isolation system on the response of structures subjected to harmonic ground excitation so as to gain some insight into the dynamics of the system. The ground displacement in the case of harmonic motion can be expressed as

$$u = U e^{i\omega t} \quad (3.1)$$

from which it follows that

$$\mathbf{f} = \mathbf{F} e^{i\omega t} \quad (3.2)$$

where the only nonzero component of \mathbf{F} is the first one, or

$$F_1 = (k + i\omega c) U \quad (3.3)$$

In this case, the steady-state response can be written

$$\mathbf{q} = \mathbf{Q} e^{i\omega t} \quad (3.4)$$

Introducing Eqs. (3.2) and (3.4) into Eq. (2.24), we can write

$$\mathbf{Q} = D^{-1} \mathbf{F} \quad (3.5)$$

in which D is the symmetric impedance matrix

$$D = -\omega^2 M + i\omega C + K$$

$$= \begin{pmatrix} k - \omega^2(M + mL) + i\omega c & -\omega^2 M_{12} & \cdots & -\omega^2 M_{1n} & -\omega^2 M_{1n+1} \\ -\omega^2 M_{21} & \omega_1^2 - \omega^2 & \cdots & 0 & 0 \\ \vdots & \vdots & \ddots & \vdots & \vdots \\ -\omega^2 M_{n1} & 0 & \cdots & \omega_{n-1}^2 - \omega^2 & 0 \\ -\omega^2 M_{n+11} & 0 & \cdots & 0 & \omega_n^2 - \omega^2 \end{pmatrix} \quad (3.6)$$

For given beam parameters and excitation amplitude and frequency, the response depends on the isolation system parameters M , c and k only.

Equation (3.5) can be rewritten as

$$\mathbf{Q} = \frac{(\text{Cof } D)^T}{|D|} \mathbf{F} \quad (3.7)$$

where $|D|$ is the determinant of D . We recall that the matrix of cofactors is defined as

$$(\text{Cof } D)_{ij} = (-1)^{i+j} m_{ij} \quad (3.8)$$

in which m_{ij} are the minor determinants of D , so that Eq. (3.7) can be written in the more explicit form

$$\mathbf{Q} = \frac{(k + i\omega c)U}{|D|} \begin{pmatrix} m_{11} \\ -m_{12} \\ m_{13} \\ \vdots \\ (-1)^{n+2} m_{1n+1} \end{pmatrix} \quad (3.9)$$

where

$$m_{11} = \prod_{s=1}^n (\omega_s^2 - \omega^2) \quad (3.10 a)$$

$$m_{1j} = (-1)^{j+1} \omega^2 M_{j1} \frac{\prod_{s=1}^n (\omega_s^2 - \omega^2)}{\omega_{j-1}^2 - \omega^2}, \quad \text{for } j > 1 \quad (3.10 b)$$

Finally, introducing Eq. (3.9) into Eq. (3.4) the displacement vector can be written as

$$\mathbf{q} = R U \mathbf{v} e^{i(\omega t + \phi)} \quad (3.11)$$

in which

$$R e^{i\phi} = \frac{k + i\omega c}{|D|} \quad (3.12)$$

and \mathbf{v} is the vector of signed minors in Eq. (3.9) which is independent of M , c and k .

From Eq. (2.14) the elastic deformation of the structure relative to the base is given by

$$y(x, t) = R U \left(\sum_{j=1}^n v_{j+1} Y_j(x) \right) e^{i(\omega t + \phi)} \quad (3.13)$$

moreover, the motion of the base is

$$r(t) = R U v_1 e^{i(\omega t + \phi)} \quad (3.14)$$

Furthermore, the acceleration of a point on the beam is

$$\ddot{y}(x, t) = -\omega^2 R U \left(\sum_{j=1}^n v_{j+1} Y_j(x) \right) e^{i(\omega t + \phi)} \quad (3.15)$$

while the base acceleration is

$$\ddot{r}(t) = -\omega^2 R U v_1 e^{i(\omega t + \phi)} \quad (3.16)$$

From Eq. (3.13), we obtain the bending moment

$$M_o(x, t) = EI R U \left(\sum_{j=1}^n v_{j+1} \frac{d^2 Y_j(x)}{dx^2} \right) e^{i(\omega t + \phi)} \quad (3.17)$$

We notice that there is a single dimensionless amplitude parameter R and a single phase ϕ

for the system response.

On the other hand, from Eqs. (2.29) the equations of motion for the unisolated structure are

$$\ddot{s}_j + \omega_j^2 s_j = \frac{2mC_j U \omega^2}{\beta_j} e^{i\omega t} \quad j=1,2,\dots,n \quad (3.18)$$

The steady-state solution is

$$s_j(t) = \frac{2mC_j U \omega^2}{\beta_j(\omega_j^2 - \omega^2)} e^{i\omega t} \quad (3.19)$$

Introducing the notation

$$Rb_j = \frac{2mC_j U \omega^2}{\beta_j(\omega_j^2 - \omega^2)} \quad (3.20)$$

and using Eq. (2.14), the motion of the structure is given by

$$y(x,t) = \left(\sum_{j=1}^n Rb_j Y_j(x) \right) e^{i\omega t} \quad (3.21)$$

Comparing Eqs. (3.13) and (3.21) we conclude that Rb_j ($j=1,2,\dots,n$) is analogous to $R U v_i$ ($i=2,3,\dots,n+1$). Additionally, the acceleration of a point on the beam is

$$\ddot{y}(x,t) = -\omega^2 \left(\sum_{j=1}^n Rb_j Y_j(x) \right) e^{i\omega t} \quad (3.22)$$

The bending moment in this case is given by

$$M_o(x,t) = EI \sum_{j=1}^n Rb_j \frac{d^2 Y_j(x)}{dx^2} e^{i\omega t} \quad (3.23)$$

The amplitude parameter Rb_j defines the response in this case.

3.2 Comparative analysis of the isolated and unisolated structure response

With base isolation, we are interested in reducing the displacement, acceleration and stress in the structure and the displacement and acceleration of the base. From Eqs. (3.13)-(3.17), we observe that these quantities depend on the dimensionless amplitude parameter R only for a given structure and excitation amplitude and frequency.

Accordingly, we are interested in minimizing R which can be written as

$$R(M,c,k) = \sqrt{\frac{k^2 + \omega^2 c^2}{[a + b(k - \omega^2(M + mL))]^2 + (b\omega c)^2}} \quad (3.24)$$

after operating on Eq. (3.12). We have that

Table 3.1 Parameters of the mechanical model of the building

Section	
Ext. diameter [m]	10
Int. diameter [m]	9.5
Area moment of inertia [m ⁴]	91.054
Height [m]	30
Young's modulus [N/m ²]	25 10 ⁹
Mass density [Kg/m]	17766

$$a = \omega^2 \sum_{j=1}^n (-1)^{j+3} M_{j+1} m_{j+1}$$

$$b = m_{j+1} \quad (3.25)$$

However, this function has only a trivial minimum ($R=0$, for $c=0$ and $k=0$) that makes no sense with the physical model. Nevertheless, the function has a maximum ($R=1/b$, for $M=(a/b\omega^2)-mL$ and $k=0$).

Consequently, we are confined to ask just for small parameters c and k . This smallness has limits however, defined by wind load consideration which is important on designing isolated structures. In addition, the basement mass can be chosen so as to avoid the maximum of R .

At this point, we need to define the parameters of the building's mechanical model to carry out an engineering design for wind load to determine k and c , and then, to obtain and compare the response of the isolated and unisolated structures. We study a concrete structure with annular section that models a 10-story building, which is defined in Table 3.1.

A simple isolation system design that limits the base horizontal displacement under wind load was carried out. The analysis was static and did not consider base rotation. The results for k and c are:

$$k = 4.5 \cdot 10^5 \text{ N/m} \quad c = 10^5 \text{ N s/m} \quad (\zeta=0.1)$$

We need also to define the number of cantilever eigenfunctions n involved in the analysis, we choose $n=5$ to study this system. Table 3.2 shows results from solving Eq. (2.17) numerically and using Eq. (2.20), and results for C_j . Note that the ω_j are not natural frequencies of the isolated structure, but of the unisolated one.

We have to define also the excitation frequency ω . We select this frequency out of the range of dominant frequencies in power spectra of ground displacement for common

Table 3.2 Modal parameters of the building

ω_1 [r/s]	44.2
ω_2	277.1
ω_3	776.0
ω_4	1520.6
ω_5	2513.7
C_1	$10.055 \cdot 10^{-4}$
C_2	$13.951 \cdot 10^{-4}$
C_3	$13.687 \cdot 10^{-4}$
C_4	$13.698 \cdot 10^{-4}$
C_5	$13.702 \cdot 10^{-4}$

earthquakes, although it is difficult to find those spectra since most of the measured spectra are of acceleration. We choose $\omega=2.0$ r/s as a representative value. We set the amplitude of the ground displacement $U=0.1$ m.

The only parameter not defined thus far is the mass of the base. The value of this parameter depends on engineering considerations mainly; and on the fact that the function R , now $R(M)$ only, attains a maximum for $M=(k+a/b)/\omega^2 - mL$. In Fig. 3.1 we can see the variation of R as M changes. In this case the maximum of the curve is in the negative range of M ; if ω were lower the peak could be in the positive range. Using engineering considerations and these plots M can be chosen; we select M as 40,000 Kg. Again, if ω were lower this choice would be more critical.

Now we can carry out the performance comparison between the isolated and the unisolated buildings. The results (absolute values) for the comparable amplitude parameters $R U v_i$, that is called Ra_i , and Rb_j are shown in Table 3.3 where U has been included for comparison with Ra_1 , the base amplitude.

As we see from these results, the amplitude parameters Ra_i are smaller than their unisolated counterparts Rb_j ; moreover, the base absolute amplitude of motion is lower than the amplitude of the ground motion. Therefore, the isolated structure performs better in all senses. We can show however, that if M is chosen near a value it renders R maximum (M near zero in this case) we may not get these reductions relative to the unisolated buildings; in fact, we could get amplifications. This is easily seen by evaluating R at the critical value of M ($(k+a/b)/\omega^2 - mL$) and comparing with R evaluated at $c=k=\infty$ (unisolated structure) in

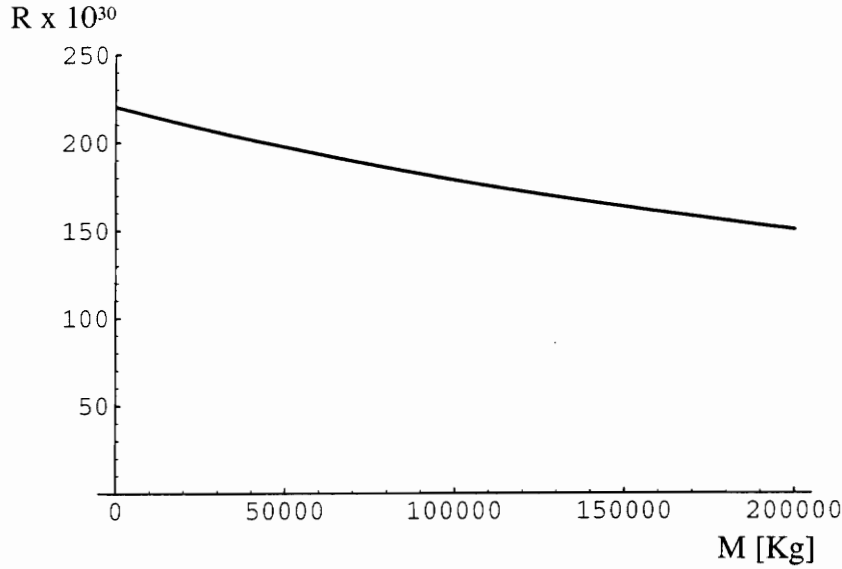


Figure 3.1 Amplitude parameter R as a function of base mass

Table 3.3. Results of the amplitude parameters Ra_i and Rb_j

i	Ra_i [m]	j	Rb_j [m]
1	.02654	U=0.10	
2	.03110	1	.11716
3	.00044	2	.00165
4	.00003	3	.00012
5	.00001	4	.00002
6	0	5	00001

Eq. (3.24), which gives respectively

$$\sqrt{\left(\frac{k}{\omega cb}\right)^2 + \frac{1}{b^2}} > \frac{1}{b}$$

It is also seen from the plot that if we augment M we obtain additional reduction in the response.

However, we find that the analysis carried out before is strongly dependent on ω ; as a consequence, the conclusions reached apply for exciting frequencies near $\omega=2$ r/s. We will not present here the analysis done with ω as variable since in the next chapter we study the actual random input; nonetheless, we can state conclusions reached through that analysis. If we reduce ω the plots $R(M)$ keep their shape, but augment and move to the right; consequently, the response amplitudes are larger and the base mass is likely to be

near critical M . As a result, the dynamic and stress amplitudes may be larger in the isolated case than in the unisolated one, as it was shown. That being the case, we find that damping helps greatly in reducing the amplitudes in this near “resonant” condition, as expected.

4. RESPONSE TO RANDOM EXCITATION

4.1 Analysis

In this chapter, we compare the response of the isolated and unisolated structures subjected to stationary random earthquake excitation. The analysis is carried out in the frequency domain, so that we compare the mean value and standard deviation of the base displacement r , of the modal amplitudes s_j , of the base acceleration \ddot{r} and of the modal accelerations \ddot{s}_j . They characterize in a probabilistic sense the structure's dynamics (Eq.(2.14)) and stresses (Eq.(2.31)), thus permitting a performance comparison.

First, we wish to recast the equations of motion of the isolated structure, Eq. (2.24), in state form. To this end, we define the $2(n+1)$ -dimensional state vector $\mathbf{x} = (\mathbf{q}^T \quad \dot{\mathbf{q}}^T)^T$. Then, the state equations have the familiar form

$$\dot{\mathbf{x}} = \mathbf{A}\mathbf{x} + \mathbf{B}\mathbf{f} \quad (4.1)$$

where

$$\mathbf{A} = \begin{pmatrix} 0 & I \\ -M^{-1}K & -M^{-1}C \end{pmatrix} \quad \mathbf{B} = \begin{pmatrix} 0 \\ M^{-1} \end{pmatrix} \quad (4.2 \text{ a,b})$$

are coefficient matrices, in which 0 and I are the $(n+1) \times (n+1)$ null and identity matrices, respectively.

We are interested in the mean value and standard deviation of q_i and its second derivatives. The mean of the state vector \mathbf{m}_x is expressed as (Ref. 5)

$$\mathbf{m}_x(t) = \int_{-\infty}^t \Phi(t-\tau) \mathbf{B} \mathbf{m}_f(\tau) d\tau \quad (4.3)$$

where $\Phi(t)$ is the transition matrix of the system and \mathbf{m}_f is the mean of the force vector. The latter can be set equal to zero vector, because the mean of the force vector depends only on $\ddot{u} + k u$, which can be assumed zero in view of actual earthquake records. Then, we obtain our first result as

$$\mathbf{m}_x = \mathbf{0} \quad (4.4)$$

it follows that

$$\mathbf{m}_{\ddot{q}} = \mathbf{0} \quad (4.5)$$

so that the mean value of the modal amplitudes, the base displacement and their first and

second derivatives is zero.

To obtain the standard deviation of q_i and its second derivative, we must first calculate the power spectral density matrix $S_{xx}(\omega)$ of the state vector, which can be expressed as (Ref. 5)

$$S_{xx}(\omega) = H^*(\omega) S_{ff}(\omega) H^T(\omega) \quad (4.6)$$

where $H(\omega)$ is the $2(n+1) \times (n+1)$ frequency response matrix of the system and $S_{ff}(\omega)$ is the $(n+1) \times (n+1)$ power spectral density matrix of the force vector.

The frequency response matrix of the system is

$$H = (i\omega I - A)^{-1} B \quad (4.7)$$

where I is the $2(n+1) \times 2(n+1)$ identity matrix. The force vector power spectral density matrix requires more elaboration. This matrix is the inverse Fourier transform of the force vector correlation matrix $R_{ff}(\tau)$. Because only the first element of the force vector is different from zero, the excitation power spectral density matrix has the form

$$S_{ff} = \begin{pmatrix} S_{f_1 f_1} & 0 & \cdots & 0 & 0 \\ 0 & 0 & \cdots & 0 & 0 \\ \vdots & \vdots & \ddots & \vdots & \vdots \\ 0 & 0 & \cdots & 0 & 0 \\ 0 & 0 & \cdots & 0 & 0 \end{pmatrix} \quad (4.8)$$

Now, the force vector's first element autocorrelation function $R_{f_1 f_1}$ is expressed

$$R_{f_1 f_1}(\tau) = \lim_{T \rightarrow \infty} \frac{1}{T} \int_{-T/2}^{T/2} [\dot{c}u(t) + ku(t)][\dot{c}u(t + \tau) + ku(t + \tau)] dt \quad (4.9)$$

Expanding we have

$$R_{f_1 f_1} = c^2 R_{\ddot{u}\ddot{u}}(\tau) + k^2 R_{uu}(\tau) + ck R_{\ddot{u}u}(\tau) + ck R_{u\ddot{u}}(\tau) \quad (4.10)$$

so that

$$S_{f_1 f_1} = c^2 S_{\ddot{u}\ddot{u}}(\omega) + k^2 S_{uu}(\omega) + ck[S_{\ddot{u}u}(\omega) + S_{u\ddot{u}}(\omega)] \quad (4.11)$$

Because the sum in the last term is zero (Ref. 5), we have finally

$$S_{f_1 f_1} = c^2 S_{\ddot{u}\ddot{u}} + k^2 S_{uu} \quad (4.12)$$

The velocity and displacement power spectral density functions of the ground, $S_{\ddot{u}\ddot{u}}(\omega)$ and $S_{uu}(\omega)$ respectively, are defined using the Clough-Penzien model (Ref. 6). This model is a representation of the power spectral density function of ground acceleration during earthquakes. It is a modification of the Kanai-Tajimi model (Ref. 5) which represents the horizontal motion of the ground as the motion of a linear oscillator subjected to white noise, i.e., the movement of the ground near the structure is approximated as a filtered white noise excitation generated deep in the ground according to simple seismic theory. The Kanai-Tajimi model is expressed as

$$S_{\ddot{u}\ddot{u}}(\omega) = \frac{4\zeta_g^2 \omega_g^2 \omega^2 + \omega_g^4}{\omega^4 + (4\zeta_g^2 - 2)\omega_g^2 \omega^2 + \omega_g^4} S_o \quad (4.13)$$

where ζ_g and ω_g are the parameters of the linear ground filter that represents the medium between the subsoil and the structure, and S_o is the intensity of the subsoil white noise signal. However, this representation does not model correctly in the very low frequency range; in fact, $S_{\ddot{u}\ddot{u}}$ and S_{uu} are unbounded at $\omega=0$. Clough and Penzien (Ref. 6) proposed a modification through the addition of a high pass linear filter to the model that eliminates the singularities. The Clough-Penzien model can be written as

$$S_{\ddot{u}\ddot{u}}(\omega) = \frac{4\zeta_g^2 \omega_g^2 \omega^2 + \omega_g^4}{\omega^4 + (4\zeta_g^2 - 2)\omega_g^2 \omega^2 + \omega_g^4} \frac{\omega^4}{\omega^4 + (4\zeta_c^2 - 2)\omega_c^2 \omega^2 + \omega_c^4} S_o \quad (4.14)$$

where ω_c and ζ_c are the parameters of the additional filter with which actual spectra are better represented in the low frequency range.

The spectral functions in Eq. (4.12) can be calculated using the derivative relations for these functions (Ref. 5), namely,

$$S_{\ddot{u}\ddot{u}} = \frac{S_{\ddot{u}\ddot{u}}}{\omega^2} \quad , \quad S_{uu} = \frac{S_{\ddot{u}\ddot{u}}}{\omega^4} \quad (4.15)$$

Accordingly, we have that

$$S_{f_i f_i}(\omega) = \frac{4\zeta_g^2 \omega_g^2 \omega^2 + \omega_g^4}{\omega^4 + (4\zeta_g^2 - 2)\omega_g^2 \omega^2 + \omega_g^4} \frac{1}{\omega^4 + (4\zeta_c^2 - 2)\omega_c^2 \omega^2 + \omega_c^4} (k^2 + \omega^2 c^2) S_o \quad (4.16)$$

This defines the force power spectral density matrix, Eq. (4.8), and hence the power spectral density matrix ($2(n+1) \times 2(n+1)$) of the state vector, Eq. (4.6).

At this point, we can determine the complete matrix of covariances of the generalized coordinates and their derivatives. We are primarily interested in the standard deviation of q_i , which is equal to the square root of the variance (Ref. 5), or in this zero-mean process

$$\sigma_i = \sqrt{\int_{-\infty}^{\infty} (H^* S_{ff} H^T)_{ii} d\omega} \quad (4.17)$$

which upon using Eq. (4.8) reduces to

$$\sigma_i = \sqrt{2 \int_0^{\infty} |H_{i1}|^2 S_{f_i f_i} d\omega} \quad i=1,2,\dots, n+1 \quad (4.18)$$

Moreover, the standard deviation of the generalized acceleration \ddot{q}_i has the form

$$\sigma_{a_i} = \sqrt{2 \int_0^{\infty} \omega^4 |H_{i1}|^2 S_{f_i f_i} d\omega} \quad (4.19)$$

From Eq. (2.29), the modal equations of motion of unisolated structure are

$$\ddot{s}_j + \omega_j^2 s_j = \frac{-2mC_j}{\beta_j} \ddot{u} \quad j=1,2,\dots,n \quad (4.20)$$

Because Eqs. (4.20) are independent, the analysis is simpler. We define for each equation a two-dimensional state vector $\mathbf{x}_j = (s_j \quad \dot{s}_j)^T$ and each modal state equation can be expressed as

$$\dot{\mathbf{x}}_j = A_j \mathbf{x}_j + B_j f_j \quad (4.21)$$

where

$$A = \begin{pmatrix} 0 & 1 \\ -\omega_j^2 & 0 \end{pmatrix} \quad B = \begin{pmatrix} 0 \\ 1 \end{pmatrix} \quad (4.22 \text{ a,b})$$

The mean of the state space vector in this case is

$$\mathbf{m}_{x_j} = \int_{-\infty}^t \Phi_j(t-\tau) B_j m_{f_j}(\tau) d\tau \quad (4.23)$$

Because the mean value of the ground acceleration can be assumed to be zero, it follows that

$$\mathbf{m}_{x_j} = \mathbf{0} \quad (4.24)$$

In addition,

$$\mathbf{m}_{\dot{x}_j} = \mathbf{0} \quad (4.25)$$

or, the mean value of each modal amplitude and its second derivative is zero.

The 2 x 2 power spectral density matrix $S_{x_j x_j}$ of the state vector is

$$S_{x_j x_j}(\omega) = H_j^*(\omega) S_{f_j f_j}(\omega) H_j^T(\omega) \quad (4.26)$$

where H_j is the 2 x 1 frequency response matrix

$$H_j(\omega) = (i\omega I - A_j)^{-1} B_j \quad (4.27)$$

which has the explicit form

$$H_j(\omega) = \begin{pmatrix} \frac{1}{\omega_j^2 - \omega^2} \\ i\omega \\ \frac{\omega_j^2 - \omega^2}{\omega_j^2 - \omega^2} \end{pmatrix} \quad (4.28)$$

The force power spectral density function $S_{f_j f_j}$ is the inverse Fourier transform of the force autocorrelation function $R_{f_j f_j}$, where the latter has the expression

$$R_{f_j f_j}(\tau) = \lim_{T \rightarrow \infty} \frac{1}{T} \int_{-T/2}^{T/2} \frac{4m^2 C_j^2}{\beta_j^2} \ddot{u}(t) \ddot{u}(t + \tau) dt \quad (4.29)$$

Equation (4.29) yields

$$R_{f_j f_j} = \frac{4m^2 C_j^2}{\beta_j^2} R_{\ddot{u}}(\tau) \quad (4.30)$$

where $R_{\ddot{u}}(\tau)$ is the autocorrelation function of the ground acceleration. The inverse Fourier transform of Eq. (4.30) is simply

$$S_{f_j f_j} = \frac{4m^2 C_j^2}{\beta_j^2} S_{\ddot{u}}(\omega) \quad (4.31)$$

Using the Clough-Penzien model, Eq. (4.15), we obtain

$$S_{f_j f_j}(\omega) = \frac{4\zeta_g^2 \omega_g^2 \omega^2 + \omega_g^4}{\omega^4 + (4\zeta_g^2 - 2)\omega_g^2 \omega^2 + \omega_g^4} \frac{\omega^4}{\omega^4 + (4\zeta_c^2 - 2)\omega_c^2 \omega^2 + \omega_c^4} \frac{4m^2 C_j^2}{\beta_j^2} S_o \quad (4.32)$$

The standard deviation of the modal amplitude s_j is then

$$\sigma_j = \sqrt{2 \int_0^\infty \frac{S_{f_j f_j}}{(\omega_j^2 - \omega^2)^2} d\omega} \quad j=1,2, \dots, n \quad (4.33)$$

whereas the standard deviation of the modal acceleration \ddot{s}_j is

$$\sigma_{a_j} = \sqrt{2 \int_0^\infty \frac{\omega^4 S_{f_j f_j}}{(\omega_j^2 - \omega^2)^2} d\omega} \quad (4.34)$$

4.2 Comparative analysis of the isolated and unisolated structure response

The comparison between the isolated and unisolated structure response is carried out on the building whose structural and isolation system characteristics were defined in Section 3.2. Therefore, the frequency response matrices are as defined by Eqs. (4.7) and (4.28). In addition, we must define the parameters in the Clough-Penzien representation. To this end, we use the parameters obtained by Lin, Tadjbakhsh, Papageorgiou and Ahmadi (Ref. 7) by fitting the Clough-Penzien model to the specific barrier model of Papageorgiou and Aki (Ref. 8), which represents faulting on heterogeneous planes during earthquakes, and provides a spectral representation of the ground acceleration. This model has been applied to typical California earthquakes (Ref. 9) and the results of the fitting process for a moment magnitude 6.0 earthquake (Ref. 10) are

$$\omega_g = 21.80 \text{ r/s} , \quad \zeta_g = 0.59 , \quad S_o = 0.006967 \text{ m}^2/\text{s}^3 , \quad \omega_c = 3.14 \text{ r/s} , \quad \zeta_c = 1.0$$

The ground acceleration power spectral density function, Eq. (4.14), is shown in Fig. 4.1, and the corresponding force power spectral density function $S_{f_j f_j}$, Eq.(4.16), is shown in Fig 4.2. Note the different frequency range in which they are dominant, and that in the unisolated case $S_{f_j f_j}$ is defined by $S_{\ddot{u}}$.

Letting the number n of cantilever eigenfunctions in Eq. (2.14) be equal to 4, the

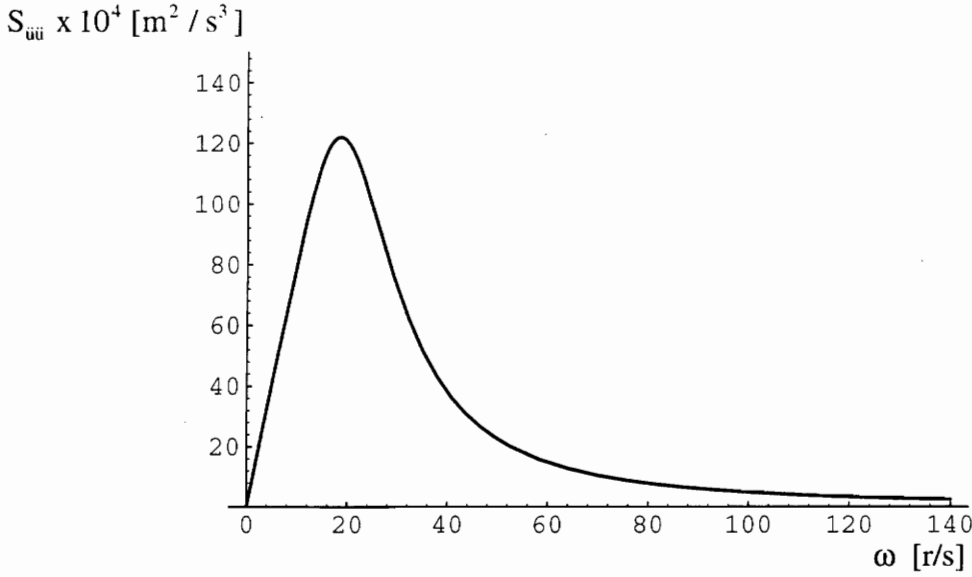


Fig. 4.1 Ground acceleration power spectral density function

standard deviations of the generalized coordinates and accelerations can be calculated by means of Eqs. (4.18), (4.19), (4.33) and (4.34). In practice, the upper limit in the integrals cannot be infinity, as actual excitation spectra die out at high frequencies. This limit is chosen as the value at which the integrand is so small that a change in the chosen limit does not affect the result.

Typical plots for the squared magnitudes of the frequency response functions H_{11} (base FRF) and H_{21} (first modal amplitude FRF) are shown in Figs. 4.3 and 4.4 respectively. The product $|H_{11}|^2 S_{f_1 f_1}$ is shown in Fig. 4.5. The area under this curve is $\sigma_1^2/2$ and can be calculated numerically. The remaining integrands $|H_{i1}|^2 S_{f_1 f_1}$ are shown in Figs. 4.6-4.9. The integrands for calculating the acceleration standard deviations σ_{a_1} and σ_{a_2} are shown in Figs. 4.10 and 4.11. The remaining integrands of σ_{a_i} ($i=3,4,5$) are similar to Fig. 4.11 in this frequency range.

For the unisolated case, the integrands $S_{f_j f_j} / (\omega_j^2 - \omega^2)^2$ of the modal amplitude standard deviations, are plotted in Figs. 4.12-4.15. We note that the integration for the first modal amplitude cannot be carried out, because the integrand is unbounded due to fact that the building is undamped. Additionally, Figs. 4.16 and 4.17 show the integrands of the standard deviations σ_{a_1} and σ_{a_2} . The remaining integrands of σ_{a_j} ($j=3,4$) are similar to Fig. 4.17.

The results are condensed in Tables 4.1 and 4.2. In which the ground displacement

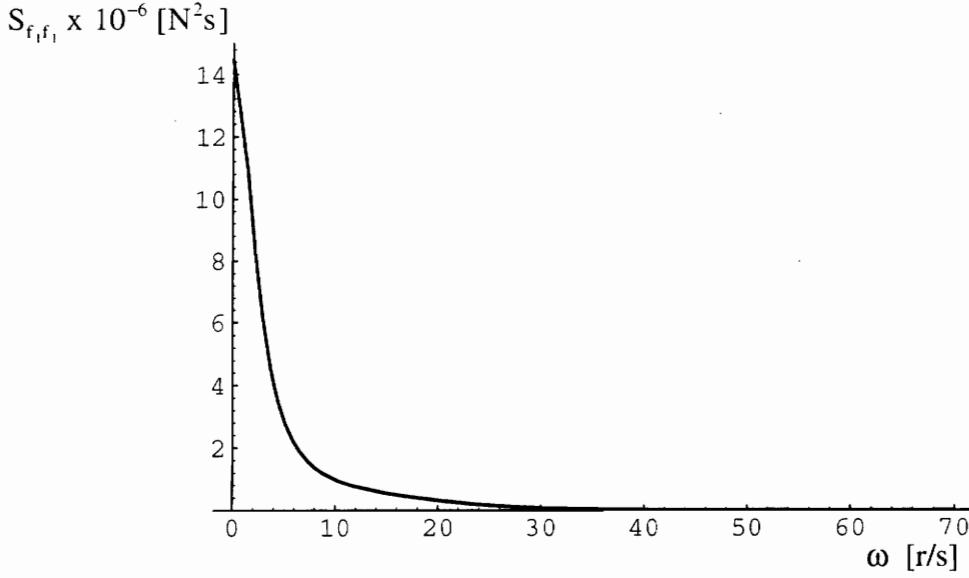


Fig. 4.2 Force power spectral density function

and acceleration standard deviations

$$\sigma_u = \sqrt{2 \int_0^{\infty} S_{uu} d\omega} \quad , \quad \sigma_{\ddot{u}} = \sqrt{2 \int_0^{\infty} S_{\ddot{u}\ddot{u}} d\omega} \quad (4.35)$$

have been included for comparison with the base displacement and acceleration standard deviations.

We can compare the performance of the isolated and unisolated structures by analyzing Tables 4.1 and 4.2. However, these tables are incomplete since the standard deviations of the first modal amplitude and its second derivative cannot be calculated in the unisolated case, as explained earlier. Consequently, we need to find some way of comparing these parameters with their isolated counterparts.

We modeled the structure as undamped, although in reality every structure has a small amount of damping. Hence, an actual plot of Fig 4.12 , for example, would have a sharply peaked shape around the resonance, but no discontinuity at this point. Note that these curves are obtained by squaring the undamped SDOF frequency response functions. In this particular case, it can be seen that if low damping is considered, the area under the curve of the attenuated Fig. 4.12 would be significantly larger than the area under the curve in Fig. 4.6 (note the scaling). Hence, the first modal amplitude standard deviation is much larger for the unisolated case. In the case of the accelerations, again, if low damping is considered, the area under the curve of a damping-adjusted Fig. 4.16 would be much larger

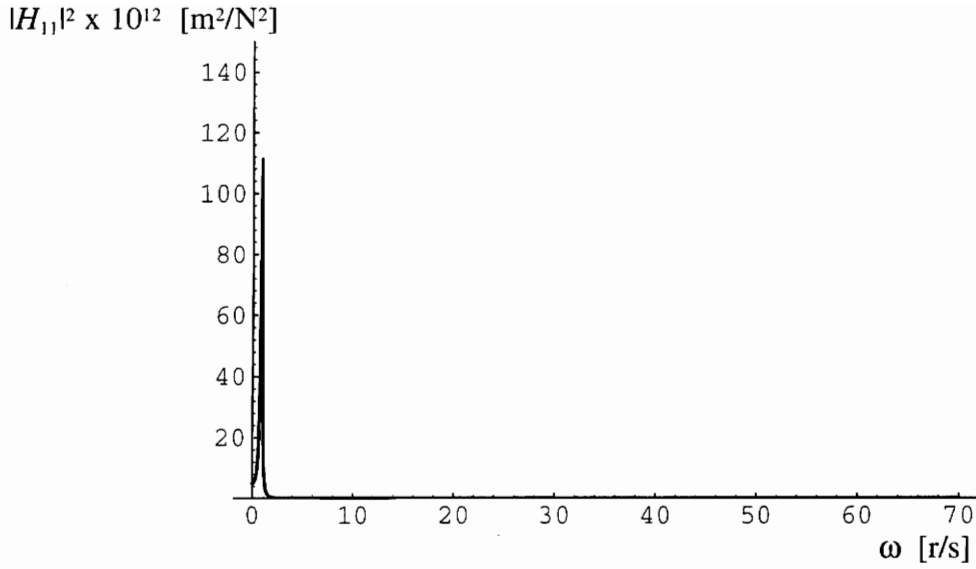


Fig. 4.3 Squared magnitude of H_{11}

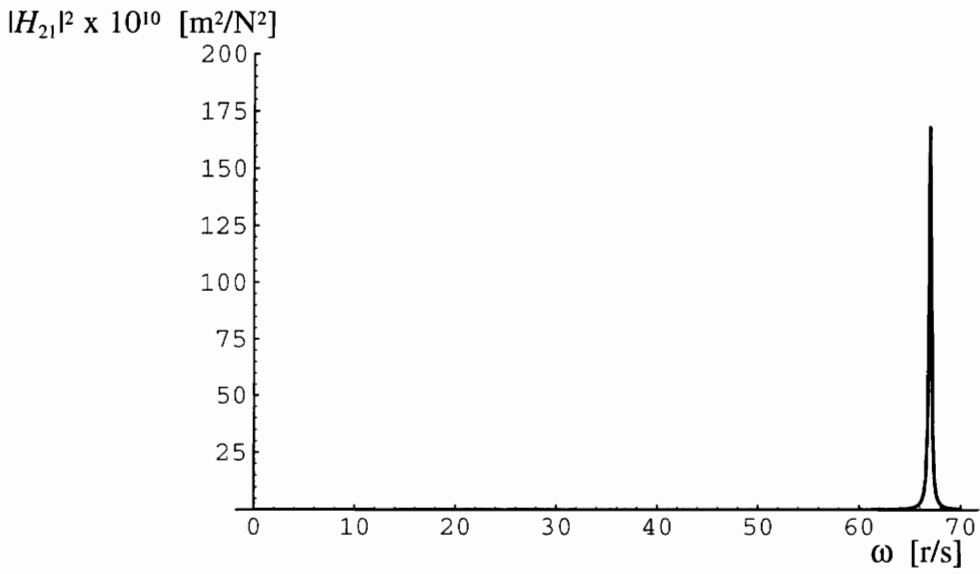


Fig. 4.4 Squared magnitude of H_{12}

than the counterpart in Fig. 4.11.

From Tables 4.1 and 4.2 we conclude that, in a probabilistic sense, the displacement, acceleration and stress levels along the beam are smaller than the levels on the unisolated or conventional building. Furthermore, the acceleration levels of the base are lower than the ground acceleration levels. It is important to note that these reductions are a

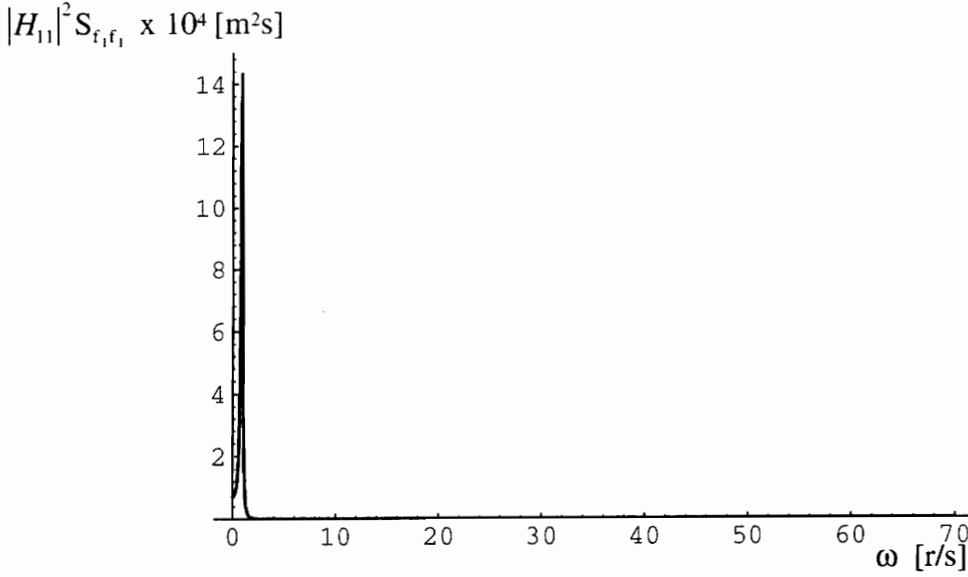


Fig. 4.5 Integrand for the base displacement standard deviation

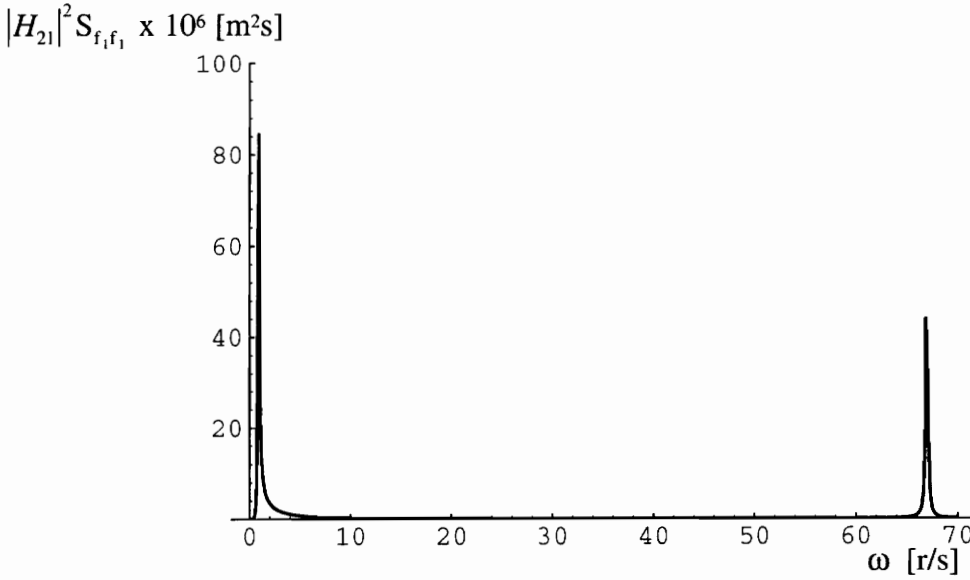


Fig. 4.6 Integrand for the first modal amplitude standard deviation

consequence of two facts. First, when a structure is isolated, the range of the dominant excitation frequencies is reduced with respect to the unisolated case and is moved toward the lower frequencies and away from the resonant frequencies of the beam, as can be seen from Figs. 4.1 and 4.2. In contrast, in the unisolated case, the excitation frequency range is broad in the range in which the frequency response functions are swelling before the single

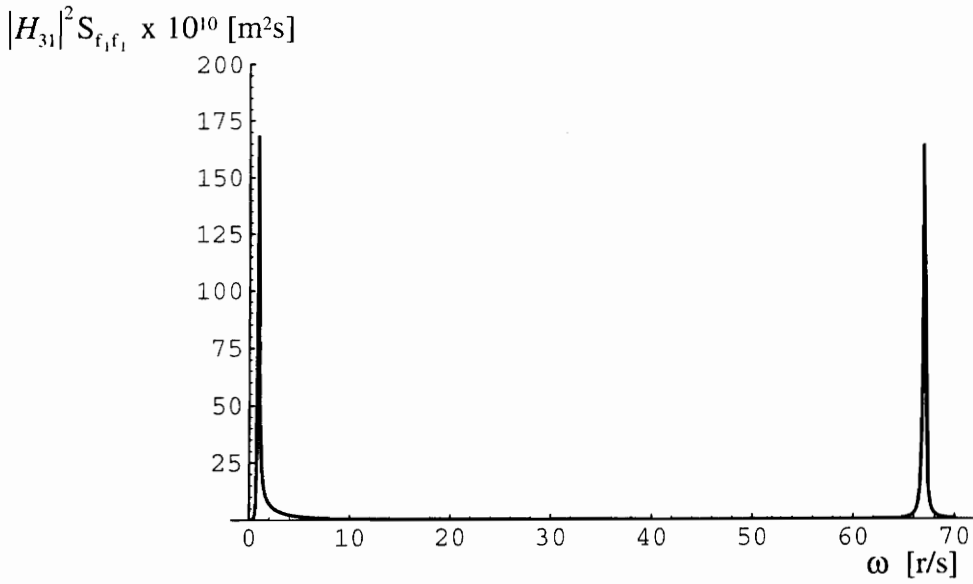


Fig. 4.7 Integrand for the second modal amplitude standard deviation

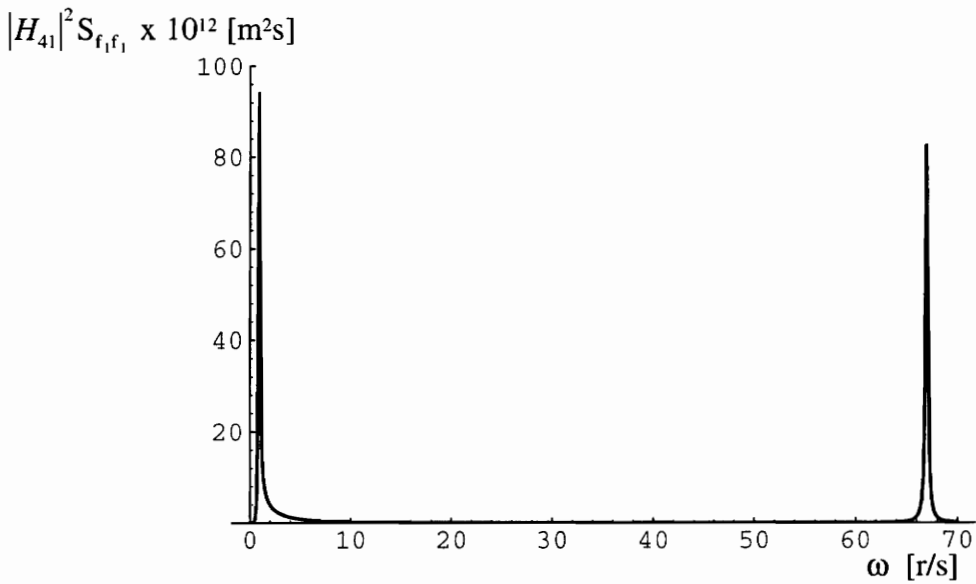


Fig. 4.8 Integrand for the third modal amplitude standard deviation

resonant frequency for each modal coordinate and acceleration. In the second place, the magnitude of the frequency response of the isolated structure is smaller than the unisolated counterpart. However, the displacement level of the base is larger than the ground displacement level, because the first natural frequency of the isolated structure is excited by the dominant range of the force spectrum. Here, damping comes into play; Tables 4.3 and

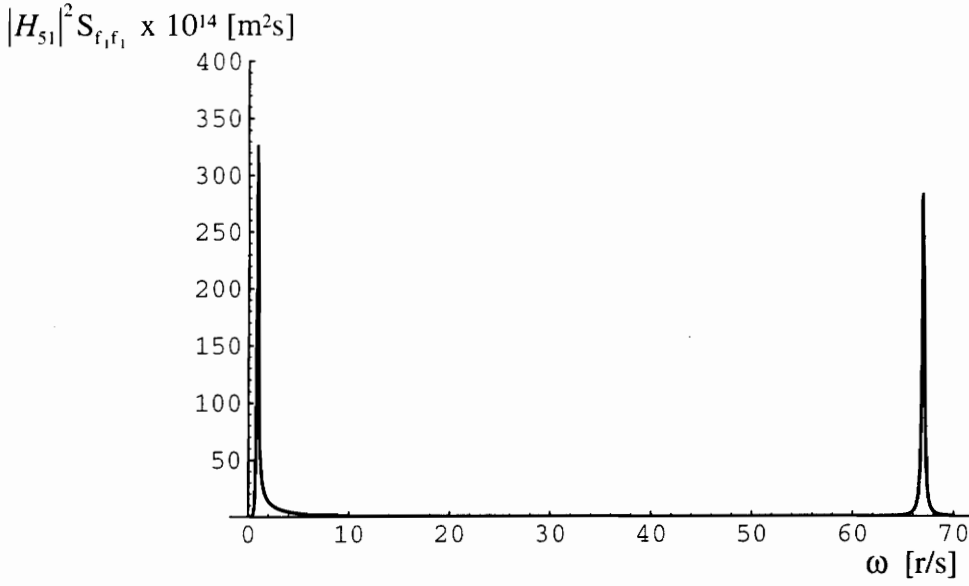


Fig. 4.9 Integrand for the fourth modal amplitude standard deviation

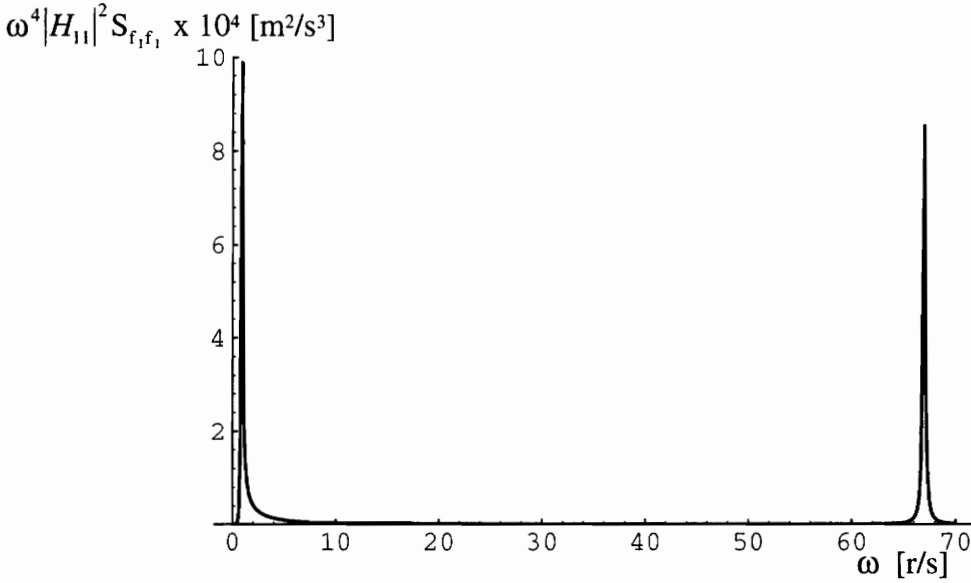


Fig. 4.10 Integrand for the base acceleration standard deviation

4.4 show the results with a double damping factor ($\zeta=0.2$) in the isolation system. As can be seen, all the standard deviation are further reduced. In particular, we note that the base displacement standard deviation is now about the same as the ground displacement standard deviation.

In the above calculations, we used $\omega=100$ r/s as the upper limit frequency in the

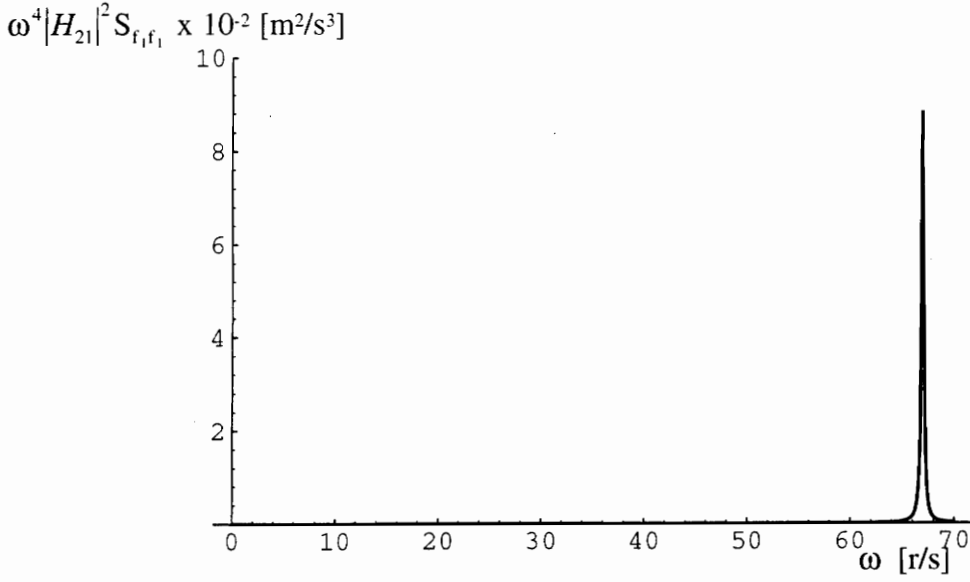


Fig. 4.11 Integrand for the standard deviation of \ddot{q}_2

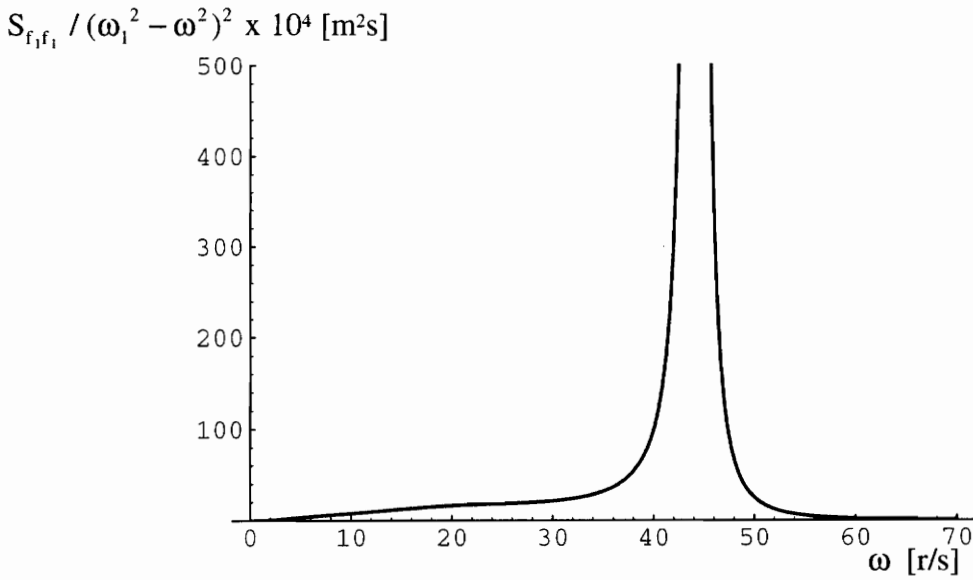


Fig. 4.12 Integrand for the first modal amplitude standard deviation (unisolated)

integrals. This choice is not critical in the calculation of the standard deviation of the displacements and accelerations for the isolated case, or displacements in the unisolated case, because small variations do not yield different results, as the area under the curve is negligible in this range. Furthermore, actual spectra does not present contribution for higher frequencies. However, in the calculation of modal acceleration standard deviations

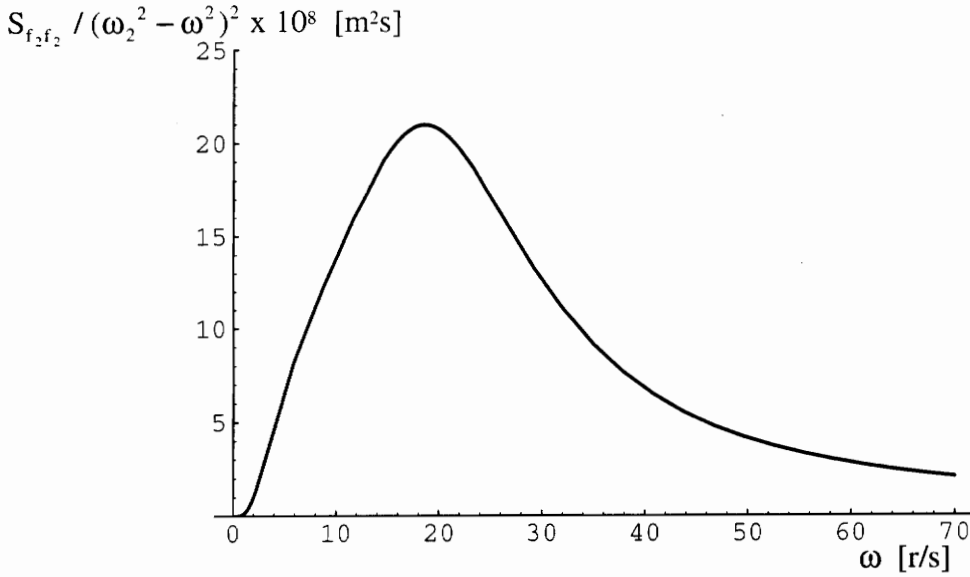


Fig. 4.13 Integrand for the second modal amplitude standard deviation (unisolated)

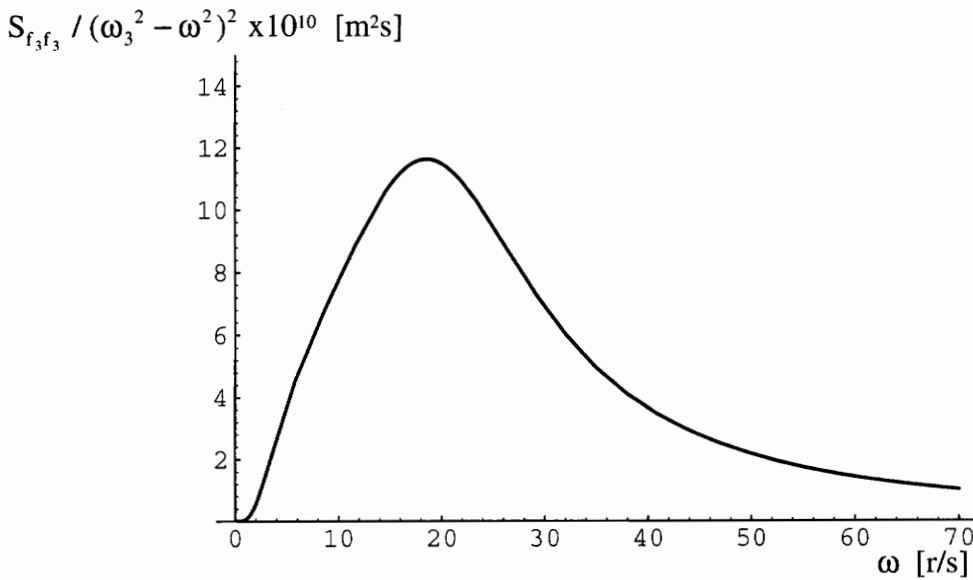


Fig. 4.14 Integrand for the third modal amplitude standard deviation (unisolated)

in the unisolated case, this matter is critical, as can be concluded from Fig. 4.17. As Clough and Penzien concluded, from an analysis of the resulting unbounded ground velocity and displacement spectra, the Kanai-Tajimi model is not a correct representation in the low frequency range; using an analysis of the acceleration response, we also note that the Clough-Penzien model is not a satisfactory representation at high frequencies. In view

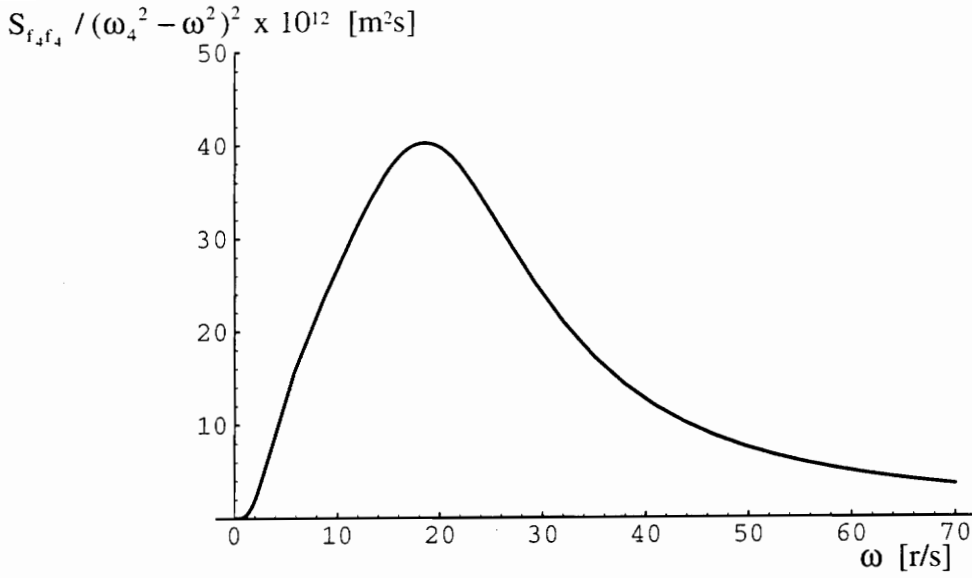


Fig. 4.15 Integrand for the fourth modal amplitude standard deviation (unisolated)

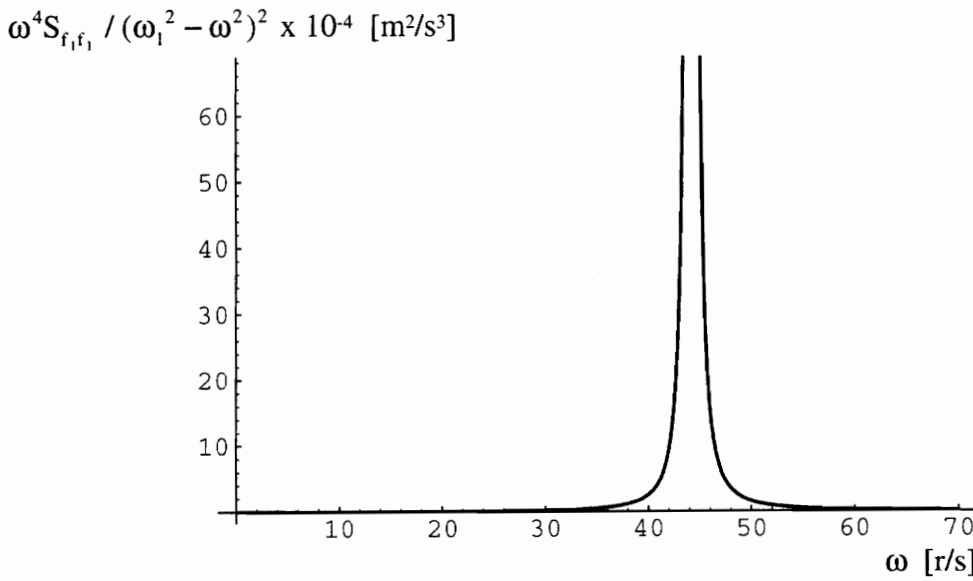


Fig. 4.16 Integrand for the standard deviation of \ddot{s}_1 (unisolated)

of actual spectra, the curve in Fig 4.17, for example, should begin to decay around 70 r/s and should not have any contribution at frequencies larger than 100 r/s. Therefore, the model requires yet another filter. In this case, a smooth low pass filter that attenuates even more the spectra at high frequencies, and thus permits a more accurate representation of actual ground acceleration spectra. Returning to our problem, we note that, in the

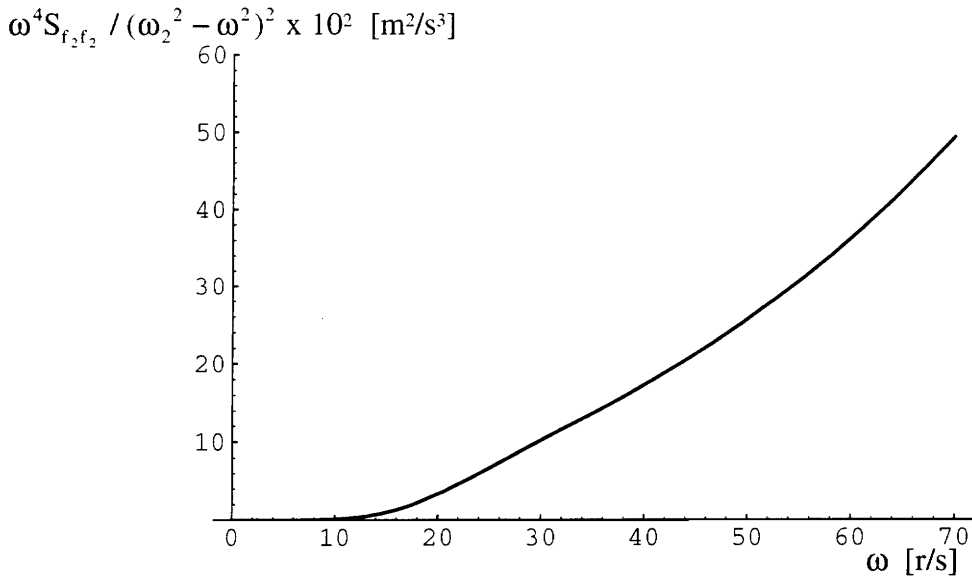


Fig. 4.17 Integrand for the standard deviation of \ddot{s}_2 (unisolated)

Table 4.1 Standard deviation of the generalized displacements

\underline{i}	<u>Isolated</u> σ_i [m]	\underline{j}	<u>Unisolated</u> σ_j [m]
1	0.030166		$\sigma_u = 0.019090$
2	0.010578	1	larger
3	0.000170	2	0.003657
4	0.000012	3	0.000269
5	0.000002	4	0.000050

Table 4.2 Standard deviation of the generalized accelerations

\underline{i}	<u>Isolated</u> σ_{a_i} [m/s ²]	\underline{j}	<u>Unisolated</u> σ_{a_j} [m/s ²]
1	0.040		$\sigma_{\ddot{u}} = 0.872$
2	28.791	1	larger
3	0.559	2	8.310
4	0.040	3	0.578
5	0.007	4	0.107

Table 4.3 Standard deviation of the generalized displacements (double ζ)

i	<u>Isolated σ_i [m]</u>
1	0.021393
2	0.008137
3	0.000128
4	0.000009
5	0.000002

Table 4.4 Standard deviation of the generalized accelerations (double ζ)

i	<u>Isolated σ_{a_i} [m/s²]</u>
1	0.030
2	20.355
3	0.396
4	0.028
5	0.005

calculations of σ_{a_i} for the unisolated case, we apply a straight low-pass filter with cut off frequency 100 r/s. As a consequence, these calculations are only approximate, because the proposed new filter should be smooth so as to model actual spectra.

5. SUMMARY AND SUGGESTIONS FOR FURTHER WORK

5.1 Summary

The damaging effects of earthquakes on structures can be mitigated by means of base isolation, which involves erecting the structure on a massive slab mounted on soft supports so as to isolate the structure from the ground motions. In this thesis, an analysis of the effectiveness of base isolation has been carried out via a comparison of earthquake response of isolated and unisolated structures. To this end, a continuous structural model has been used, namely, an Euler-Bernoulli beam. The base isolation system was modeled as linear and, more importantly, the motion of the base was measured relative to an inertial space, which is fundamental in evaluating base isolation. The earthquake excitation has been represented as an stationary stochastic process. In particular, the ground acceleration spectrum was represented by the Clough-Penzien model.

The performance criteria for comparison have been defined in terms of displacement, acceleration and stress levels along the building, and displacement and acceleration of the base. The frequency domain approach permits a comparison of the response in terms of the standard deviation of the generalized coordinates and their second time derivatives.

The results have showed that an isolated structure undergoes lower levels of overall response than the nonisolated counterpart and that energy dissipation in the isolation system is essential in controlling the displacement of the base.

5.2 Suggestions for further work

The continuous model can be refined by modeling the structure as an assemblage of columns and beams. Floors and walls can be added to the model either as rigid or as elastic plates. The excitation can be assumed to be nonstationary, in the sense that the excitation spectrum consists of a stationary part modulated by a time varying amplitude. Of course, all these refinements in the model should be introduced one at a time, because otherwise the resulting model would not lend itself to easy analysis.

Finally, active control can be added to the isolated structure, which can result in

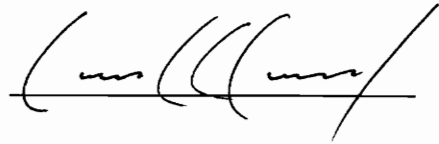
near ideal isolation, in the sense that the structure behaves as a rigid body motionless in an inertial space, while the ground moves under the base.

REFERENCES

1. Kelly, J. M., "Aseismic Base Isolation: Review and Bibliography," Soil Dynamics and Earthquake Engineering, Vol. 5, 1986, pp. 202-216.
2. Skinner, R. I., Robinson, W. H. and McVerry, G. H., An Introduction to Seismic Isolation, John Wiley & Sons, England, 1993. TA 618.64 S53 1993
3. Meirovitch, L., Analytical Methods in Vibrations, Macmillan Publishing Co., New York, 1967.
4. Meirovitch, L., Elements of Vibration Analysis, 2nd Edition, McGraw-Hill, Mexico, 1986
5. Soong, T. T. and Grigoriu, M., Random Vibration of Mechanical and Structural Systems, Prentice-Hall International, U.S.A., 1993.
6. Clough, R. W. and Penzien, J., Dynamics of Structures, MacGraw-Hill, U.S.A., 1975.
7. Lin, B. C., Tadjbakhsk, I. G., Papageorgiou, A. S. and Ahmadi, G., "Response of Base-Isolated Buildings to Random Excitation Described by the Clough-Penzien Spectral Model," Earthquake Engineering and Structural Dynamics, Vol. 18, pp. 49-62, 1989.
8. Papageorgiou, A. S. and Aki, K., "A Specific Barrier Model for the Quantitative Description of Inhomogeneous Faulting and the Prediction of Strong Ground Motion. Part I. Description of the Model," Bulletin of the Seismological Society of America, Vol. 73, pp. 693-722, 1983.
9. Papageorgiou, A. S. and Aki, K., "A Specific Barrier Model for the Quantitative Description of Inhomogeneous Faulting and the Prediction of Strong Ground Motion. Part II. Applications of the Model," Bulletin of the Seismological Society of America, Vol. 73, pp. 953-978, 1983.
10. Naeim, F., The Seismic Design Handbook, Van Nostrand Reinhold, New York, 1989.

VITA

The author was born to Agustín Morales and Virginia Velasco on March 18, 1969 in Puno, Perú, ashore the Lake where the Inca's empire was born. He moved to Venezuela, Land of South America's Liberator Simón Bolívar, in 1975 and is a Venezuelan citizen since 1982. He received a Mechanical Engineer degree, Cum Laude, from Universidad Simón Bolívar, Caracas, in October 1991. He immediately joined the Mechanics Department in that institution, and was awarded a joint scholarship from Fundación Sivensa and his University in 1993 to pursue the Master of Science degree in Engineering Mechanics at Virginia Polytechnic Institute and State University. He received an scholarship from the Organization of American States to continue studies towards the Doctor of Philosophy degree in the same program beginning in August 1995.

A handwritten signature in black ink, consisting of stylized cursive letters, positioned above a horizontal line.

César A. Morales V.